

A new damage index for detecting sudden change of structural stiffness

B. Chen[†] and Y. L. Xu[‡]

*Department of Civil and Structural Engineering, The Hong Kong Polytechnic University,
Kowloon, Hong Kong*

(Received March 30, 2006, Accepted November 20, 2006)

Abstract. A sudden change of stiffness in a structure, associated with the events such as weld fracture and brace breakage, will cause a discontinuity in acceleration response time histories recorded in the vicinity of damage location at damage time instant. A new damage index is proposed and implemented in this paper to detect the damage time instant, location, and severity of a structure due to a sudden change of structural stiffness. The proposed damage index is suitable for online structural health monitoring applications. It can also be used in conjunction with the empirical mode decomposition (EMD) for damage detection without using the intermittency check. Numerical simulation using a five-story shear building under different types of excitation is executed to assess the effectiveness and reliability of the proposed damage index and damage detection approach for the building at different damage levels. The sensitivity of the damage index to the intensity and frequency range of measurement noise is also examined. The results from this study demonstrate that the damage index and damage detection approach proposed can accurately identify the damage time instant and location in the building due to a sudden loss of stiffness if measurement noise is below a certain level. The relation between the damage severity and the proposed damage index is linear. The wavelet-transform (WT) and the EMD with intermittency check are also applied to the same building for the comparison of detection efficiency between the proposed approach, the WT and the EMD.

Keywords: sudden damage; acceleration response; signal discontinuity; damage index; empirical mode decomposition; wavelet transform; damage detection.

1. Introduction

The degradation of civil engineering structures due to harsh environment may lead to a sudden change of stiffness in a structure associated with the events such as weld fracture, column buckling, and brace breakage (Johnson *et al.* 2000, Yang *et al.* 2001). Such a sudden change of stiffness in a structure will cause a discontinuity in acceleration response time histories recorded in the vicinity of damage location at damage time instant. Since most of currently used vibration-based structural damage detection methods operate with structural response data recorded before and after the occurrence of structural damage (Sohn *et al.* 2003, Maity and Tripathy 2005), they cannot be used to detect damage event on line and find out when the damage event occurs. To acquire a damage

[†] Ph.D., Research Assistant, E-mail: cb.steven@polyu.edu.hk

[‡] Ph.D., Chair Professor, Corresponding author, E-mail: ceylxu@polyu.edu.hk

feature retaining damage time instant, instantaneous damage indices and/or the application of time-frequency data processing tool for analyzing measurement data are necessary.

Hou *et al.* (1999, 2000) proposed a wavelet-based approach to identify the damage time instant and damage location of a simple structural model with breakage springs. By decomposing vibration signal in the time domain using wavelet analysis, the discontinuity in the signal will form a signal feature, termed damage spike, in the wavelet details. The damage time instant can then be identified in terms of the occurrence time of spike, and the damage location can be determined by the spatial distribution of the observed spikes. Sohn *et al.* (2004) incorporated wavelet transforms with the Holder exponent to capture the time varying nature of discontinuities. Their experimental results demonstrated that the Holder exponent could be an effective tool for identifying certain types of events that introduce discontinuities into the measured dynamic response data. The same idea for detecting sudden damage was adopted by Vincent *et al.* (1999) and Yang *et al.* (2001) but using empirical mode decomposition (EMD), developed by Huang *et al.* (1998, 1999), to decompose the vibration signal to capture the signal discontinuity. Numerical simulation carried out in their studies showed that EMD approach could also identify the damage time instant and damage location using the signal feature of damage spike. In addition to the above-mentioned numerical studies, Xu and Chen (2004) carried out experimental studies on the applicability of EMD for detecting structural damage caused by a sudden change of structural stiffness. A series of free vibration, random vibration, and earthquake simulation testes were performed on a three-story shear building model with different damage time instants and damage severities simulated. Their experimental results confirmed that the EMD approach with intermittency check could accurately identify the damage time instant and damage location. However, both the numerical study and the experimental investigation demonstrate that the relationship between damage spike amplitude and damage severity could not be given by either the WT or the EMD with intermittency check. To this end, Yang *et al.* (2004) suggested an alternative method based on the EMD with intermittency check and Hilbert transform to quantitatively detect the damage time instant and the natural frequencies and damping ratios of the structure before and after damage. However, this multi-stage method proposed by Yang *et al.* (2004) may not be suitable for online structural health monitoring applications because it needs great computation effort.

In this paper, signal discontinuities in the acceleration response time histories recorded in the vicinity of damage location due to a sudden damage event are closely examined for both single-degree-of-freedom (SDOF) systems and MDOF systems. A new instantaneous damage index is then proposed to detect the damage time instant, location, and severity of a structure due to a sudden change of stiffness. The proposed damage index is proportional to damage severity and suitable for online structural health monitoring applications. It can also be used in conjunction with the empirical mode decomposition (EMD) for damage detection without using the intermittency check. Numerical simulation using a five-story shear building as an example is executed to assess the effectiveness and reliability of the proposed damage detection approach for different types of excitation and at different levels of damage. The sensitivity of the damage index to the intensity and frequency range of measurement noise is also examined. The damage detection results from the proposed approaches are also compared with those from the WT and the EMD with intermittency check.

2. Empirical mode decomposition

As a signal processing method, the EMD can decompose any data set into several intrinsic mode functions (IMFs) by a procedure called sifting process (Huang *et al.* 1998, 1999). An IMF is defined as a function that satisfies two conditions: (1) within the data range, the number of extrema and the number of zero crossings are equal or differ at most by one; and (2) at any point, the mean value of the envelope defined by the local maxima and the envelope defined by the local minima is zero. Suppose $X(t)$ is a time history (signal) to be decomposed. The sifting process is conducted by first constructing the upper and lower envelopes of $X(t)$ by connecting its local maxima and local minima through a cubic spline. Designate the mean value of the two envelopes as $m_1(t)$ and compute the difference between the original time history and the mean value

$$h_1(t) = X(t) - m_1(t) \quad (1)$$

The component $h_1(t)$ is then examined to see if it satisfies the above-mentioned two requirements to be an IMF. If not, the sifting process is to be repeated by treating $h_1(t)$ as a new time history until $h_1(t)$ is an IMF, designated as $c_1(t)$. Then, the first IMF is separated from the original time history, giving a residue $r_1(t)$ as

$$r_1(t) = X(t) - c_1(t) \quad (2)$$

The sifting process is applied successively to each subsequent residue to obtain the subsequent IMFs until either the residue $r_n(t)$ is smaller than a predetermined value or it becomes a monotonic function. The original time history is finally expressed as the sum of the IMF components plus the final residue.

$$X(t) = \sum_{j=1}^n c_j(t) + r_n(t) \quad (3)$$

where $c_j(t)$ is the j th IMF component; n is the total number of IMF components; and $r_n(t)$ is the final residue. After the decomposition, the first IMF component obtained has the highest frequency content of the original time history while the final residue represents the component of the lowest frequency in the time history. During the sifting process, a criterion called intermittency check (Huang *et al.* 1999) can be imposed for each IMF component in order to limit its frequency content. This criterion works by specifying a frequency, termed intermittency frequency f_c , for each IMF component during its sifting process, so that the data having frequencies lower than f_c will be removed from the resulting IMF.

3. Signal feature due to sudden damage and new damage index

3.1 Signal feature due to sudden damage-SDOF system

Let us consider a SDOF system subjected to a sudden stiffness reduction under impulse excitation. The mass of the system is denoted as m , the damping ratio ξ of the system is supposed to remain unchanged before and after sudden damage, and the stiffness is denoted as k which will

have a sudden reduction at time instant t_i .

$$k = \begin{cases} k_u & (0 \leq t \leq t_i) \\ k_d & (t_i < t) \end{cases} \quad (4)$$

in which k_u and k_d are the stiffness of undamaged and damaged system, respectively. The initial velocity and displacement due to the impulse excitation are assumed to be 0 and v_0 , respectively. The circular frequency of the system before and after sudden damage can be expressed as

$$\omega_u = \sqrt{k_u/m}; \quad \omega_d = \sqrt{k_d/m} \quad (5)$$

Define a frequency reduction coefficient α that varies from 0 to 1

$$\omega_d = \alpha \cdot \omega_u \quad (0 < \alpha < 1) \quad (6)$$

The stiffness reduction can be expressed as

$$\Delta k = k_d - k_u = m(\omega_d^2 - \omega_u^2) = m\omega_u^2(\alpha^2 - 1) \quad (7)$$

The equation of motion of the SDOF system before sudden damage is

$$\ddot{y} + 2\xi\omega_u\dot{y} + \omega_u^2y = 0 \quad (8)$$

The above equation can be solved in terms of the given initial conditions, and the structural responses at time instant t_i are

$$\left. \begin{aligned} y_i &= e^{-\xi\omega_u t_i} \cdot \frac{v_0 \sin(\omega_u \sqrt{1-\xi^2} \cdot t_i)}{\omega_u \sqrt{1-\xi^2}} \\ \dot{y}_i &= e^{-\xi\omega_u t_i} \cdot \left[v_0 \cos(\omega_u \sqrt{1-\xi^2} \cdot t_i) - \frac{\xi v_0 \sin(\omega_u \sqrt{1-\xi^2} \cdot t_i)}{\sqrt{1-\xi^2}} \right] \end{aligned} \right\} \quad (9)$$

Let us take the time instant t_i as the start point of the SDOF system after sudden damage and use a new time axis $t_1 = t - t_i$. Then, the equation of motion of the system after damage becomes

$$\ddot{y}_1 + 2\xi\omega_d\dot{y}_1 + \omega_d^2y_1 = 0 \quad (10)$$

The initial conditions for Eq. (10) can be expressed as

$$\left. \begin{aligned} y_1(0) = y_i &= e^{-\xi\omega_u t_i} \cdot \frac{v_0 \sin(\omega_u \sqrt{1-\xi^2} \cdot t_i)}{\omega_u \sqrt{1-\xi^2}} \\ \dot{y}_1(0) = \dot{y}_i &= e^{-\xi\omega_u t_i} \cdot \left[v_0 \cos(\omega_u \sqrt{1-\xi^2} \cdot t_i) - \frac{\xi v_0 \sin(\omega_u \sqrt{1-\xi^2} \cdot t_i)}{\sqrt{1-\xi^2}} \right] \end{aligned} \right\} \quad (11)$$

The damping ratio of a civil engineering structure is often very small, that is, $\sqrt{1 - \xi^2} \approx 1$. Furthermore, the time interval $\Delta t_1 = t_{i+1} - t_i$ should be very small to describe the sudden stiffness reduction properly. As a result, one may have

$$\omega_d \sqrt{1 - \xi^2} \cdot \Delta t_1 \rightarrow 0 \Rightarrow \begin{cases} \cos(\omega_d \sqrt{1 - \xi^2} \cdot \Delta t_1) \rightarrow 1 \\ \sin(\omega_d \sqrt{1 - \xi^2} \cdot \Delta t_1) \rightarrow 0 \end{cases} \quad (12)$$

The relationship between the acceleration response increment and the sudden stiffness reduction can thus be given approximately as

$$\ddot{y}_{i+1} - \ddot{y}_i \approx -\frac{\Delta k}{m \omega_u} \cdot e^{-\xi \omega_u t_i} \cdot \sqrt{1 - \xi^2} \cdot v_0 \sin(\omega_u t_i \cdot \sqrt{1 - \xi^2}) \quad (13)$$

Eq. (13) reveals that the acceleration response increment is approximately linear to the sudden stiffness reduction for given initial velocity, damage instant and structural parameters before damage. If the time interval Δt_1 for sudden damage is further regarded as a fixed value, Eq. (13) indicates that the acceleration response discontinuity due to sudden stiffness reduction can be reflected by the slope of the acceleration response at damage instant.

To examine the slope of the acceleration response of the system at other time instant in addition to the damage time instant, a numerical example is discussed in the following based on the slope of acceleration

$$K_k = \frac{\ddot{y}_{k+1} - \ddot{y}_k}{\Delta t} \quad (k = 1, 2, \dots, n-1) \quad (14)$$

where $\Delta t = t_{k+1} - t_k = \Delta t_1$; and n is the total number of time interval for the whole response time history. The mass and stiffness of the SDOF system examined are $m = 1.117 \times 10^4$ kg and $k = 1.75 \times 10^5$ N/m. The damping ratio of the system is set as 2%. The SDOF system is subjected to an impulse, represented by 0.1 m/s initial velocity. The system is supposed to suffer a sudden 5% stiffness reduction at $t = 2.3$ s. The acceleration response time history is computed with a time interval of 0.002s and plotted in Fig. 1(a), and the corresponding acceleration response slope time history is depicted in Fig. 1(b) using its absolute value. It can be seen that there is a spike at the damage time instant t_i . The absolute values of acceleration response slope at the time instant t_{i-1} and the time instant t_{i+1} are much smaller than that at the damage time instant t_i .

$$|K_i| \gg |K_{i-1}|; \quad |K_i| \gg |K_{i+1}| \quad (15)$$

The above two features can not be seen at any other time instant without sudden stiffness reduction.

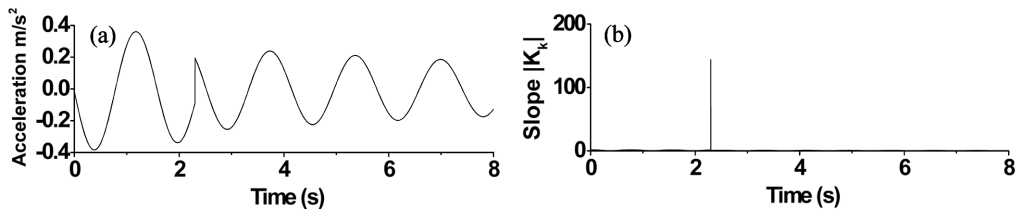


Fig. 1 Acceleration response and its slope of a SDOF system (impulse excitation)

3.2 Signal feature due to sudden damage-MDOF system

To examine the signal feature due to a sudden stiffness reduction in a multi-degree-of-freedom (MDOF) system, the acceleration responses of a five-story shear building, as shown in Fig. 2, with a sudden change of stiffness at its first story and subject to various types of external excitations are investigated numerically. The mass and horizontal stiffness of the undamaged building are uniform for all stories with a mass $m = 1.3 \times 10^6$ kg and a horizontal stiffness $k = 4.0 \times 10^9$ N/m. The Rayleigh damping assumption is adopted to construct the structural damping matrix, and the damping ratios in the first two modes of vibration of the building are set as 0.05. The original building is supposed to suffer a sudden 20% stiffness reduction in the first story with the horizontal stiffness reducing from 4.0×10^9 N/m to 3.2×10^9 N/m while the horizontal stiffness in other stories remains unchanged (no damage). Listed in Table 1 are the natural frequencies of the original and damaged building. The frequency reduction due to 20% stiffness reduction in the first story is small with a maximum reduction no more than 5% in the first natural frequency. The frequency reduction becomes even smaller in higher natural frequencies.

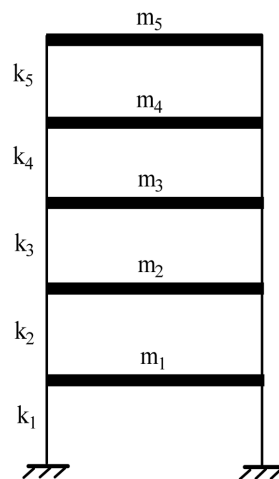


Fig. 2 Elevation of a five-story building model

Table 1 Structural frequencies before and after sudden damage

Damage extent	Frequencies (Hz)				
	f_1	f_2	f_3	f_4	f_5
0%	2.513	7.335	11.563	14.854	16.941
1%	2.508 (-0.18%)	7.324 (-0.15%)	11.55 (-0.11%)	14.85 (-0.05%)	16.94 (-0.01%)
2%	2.504 (-0.36%)	7.313 (-0.30%)	11.54 (-0.21%)	14.84 (-0.11%)	16.94 (-0.03%)
5%	2.490 (-0.94%)	7.278 (-0.78%)	11.50 (-0.53%)	14.81 (-0.26%)	16.93 (-0.07%)
10%	2.464 (-1.97%)	7.218 (-1.62%)	11.44 (-1.06%)	14.78 (-0.52%)	16.92 (-0.14%)
20%	2.407 (-4.41%)	7.088 (-3.48%)	11.32 (-2.18%)	14.71 (-1.01%)	16.90 (-0.26%)
40%	2.253 (-11.6%)	6.781 (-8.16%)	11.07 (-4.50%)	14.57 (-1.92%)	16.86 (-0.46%)

Note: Values in brackets are the percentage of change in frequency.

Three types of external excitations: seismic excitation, sinusoidal excitation, and impulse excitation, are respectively considered to compute the acceleration response of the building to have a wide collection of signal features due to sudden damage. The seismic excitation used is the first 10 second portion of the El-Centro 1940 earthquake ground acceleration (S-N component) with a peak amplitude 1.0 m/s^2 in order to reduce the computation efforts. The sinusoidal excitation is expressed by Eq. (16) and assumed to act on each floor of the building. The duration of the sinusoidal excitation is also 10 seconds.

$$f(t) = 1300 \cdot \sin(4\pi t) \quad (0 \leq t \leq 10\text{s})(\text{kN}) \tag{16}$$

The impulse excitation is supposed to occur at the first floor of the building only, represented by 0.1 m/s initial velocity of the first floor. The damage time instant of the building is set as 6.0 s for seismic excitation and sinusoidal excitation and 0.2 s for impulse excitation. The equation of motion of the building subject to a sudden reduction of 20% horizontal stiffness at its first story at the given time instant is then established for each type of external excitation, and it is solved using the Newmark- β method with a time interval of 0.002 s . The two factors in the Newmark- β method are selected as $\alpha = 1/2$ and $\beta = 1/4$.

The computed acceleration response of the first floor of the building is displayed in Fig. 3(a) for seismic excitation, in Fig. 4(a) for sinusoidal excitation, and in Fig. 5(a) for impulse excitation. It is difficult to find the signal feature due to sudden damage by direct visual inspection of the original acceleration responses. The 0.2 second portion of the acceleration response time history, containing the damage time instant, is thus expanded in Fig. 3(b) for seismic excitation and in Fig. 4(b) for

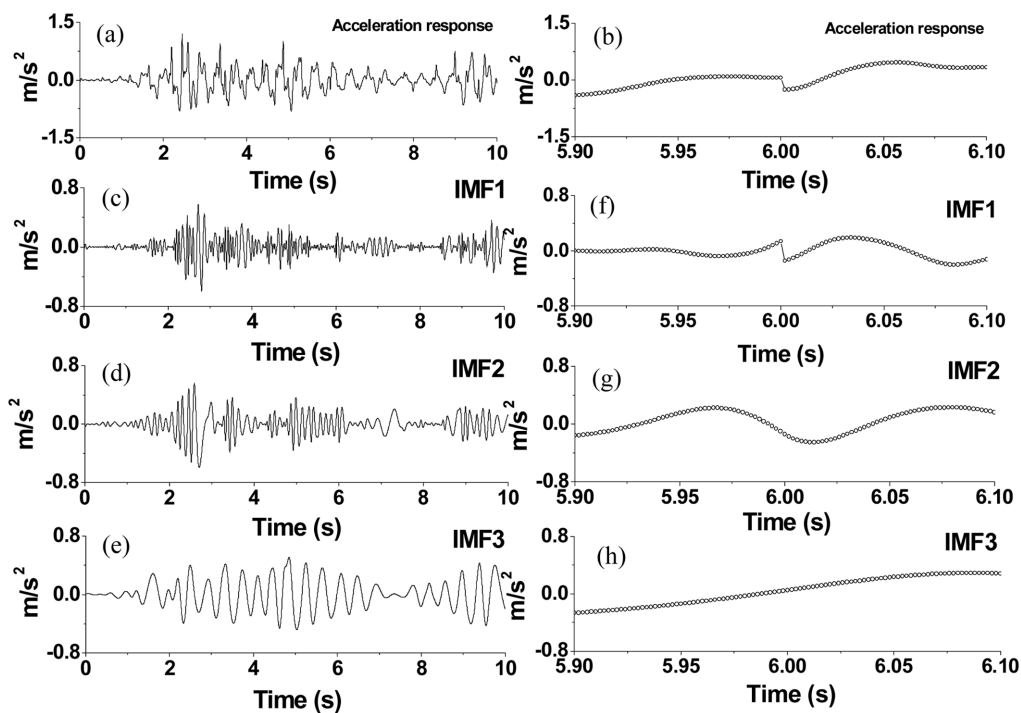


Fig. 3 Signal discontinuity due to sudden damage (seismic excitation)

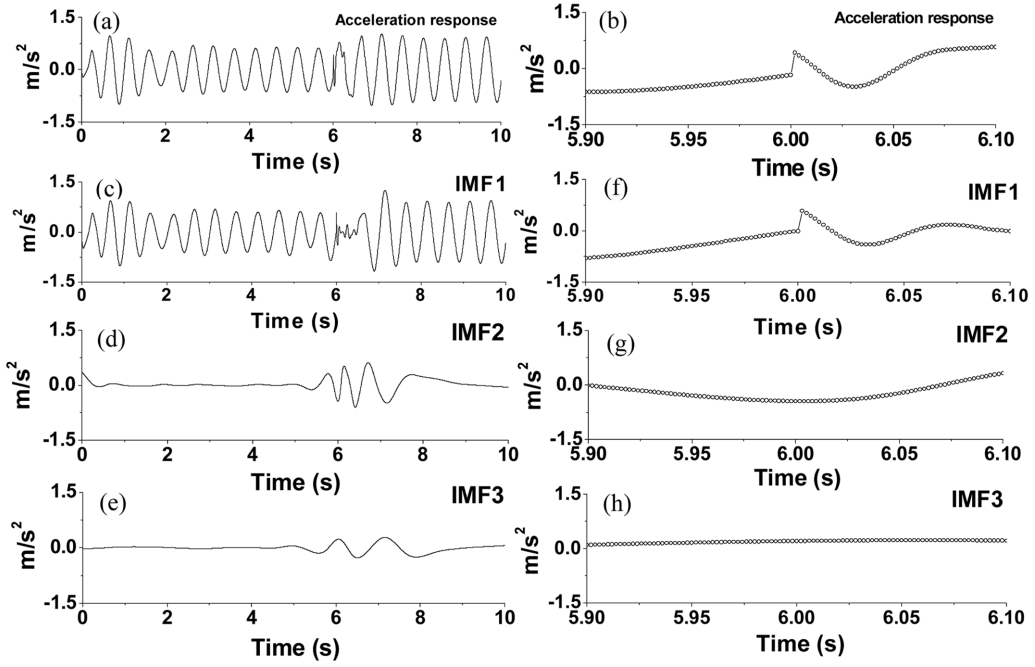


Fig. 4 Signal discontinuity due to sudden damage (sinusoidal excitation)

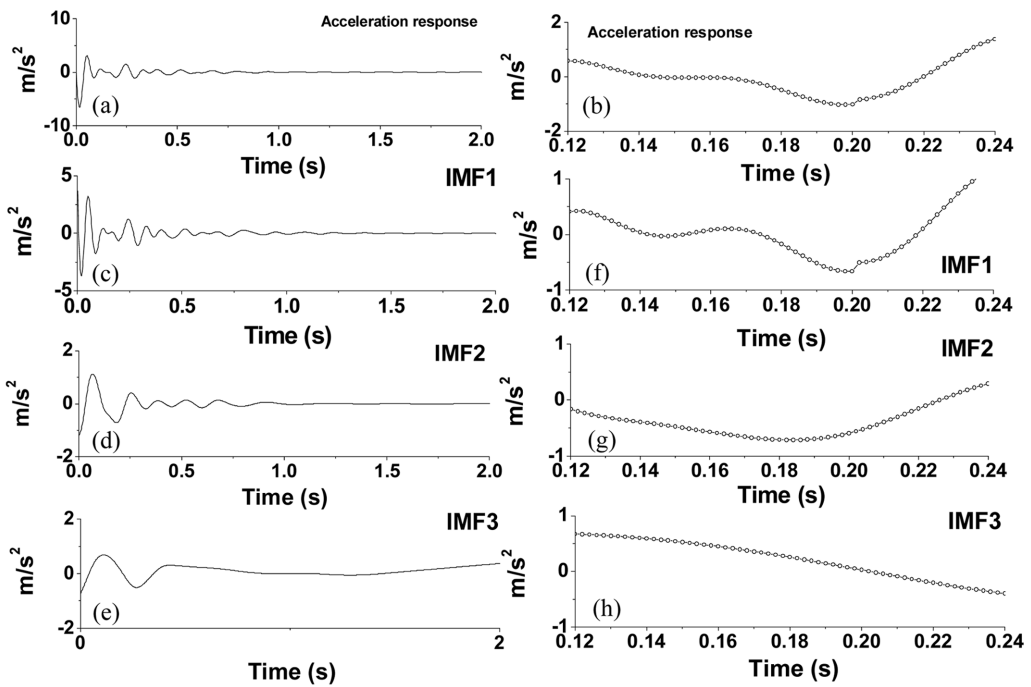


Fig. 5 Signal discontinuity due to sudden damage (impulse excitation)

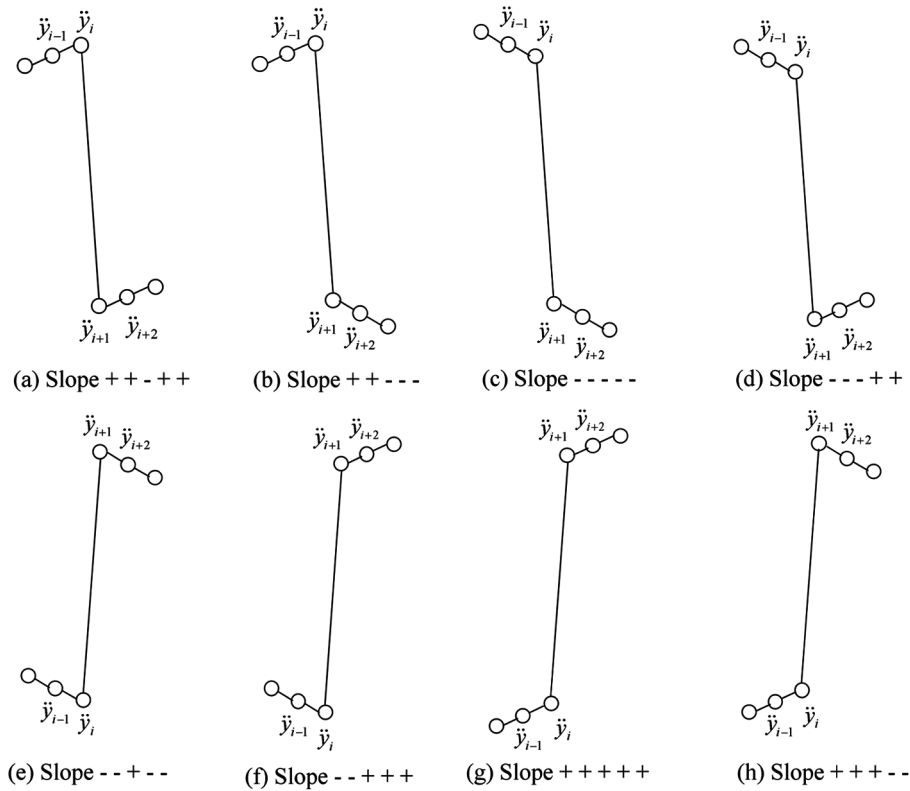


Fig. 6 Signal discontinuity patterns around damage time instant

sinusoidal excitation, and the 0.12 second portion of the same quantity is expanded in Fig. 5(b) for impulse excitation to permit a close look at signal feature due to sudden damage. It can be seen that there exists a sudden jump in the original signal at the damage time instant. The sudden reduction of horizontal stiffness of the first floor causes a clear signal discontinuity in the acceleration response time history at the damage time instant. Since the signal discontinuity is of very high frequency, the EMD is applied to decompose the original acceleration response without using intermittency check. As a result, eight, six, and six IMFs are obtained from the acceleration response time history at the first floor of the building under seismic excitation, sinusoidal excitation, and impulse excitation, respectively. Displayed in Fig. 3(c) to Fig. 3(e) are the first three IMFs of the acceleration response at the first floor of the building under seismic excitation. Similar to the original acceleration response time history, the direct visual inspection of the IMF components cannot find signal features due to sudden damage. The 0.2 second zooms of the three IMFs around the damage time instant are therefore depicted in Fig. 3(f) to Fig. 3(h). It can then be seen that the 0.2 second zoom of the first IMF is quite similar to the 0.2 second portion of the original acceleration response time history, and the signal discontinuity is reserved in the first IMF component only. This is because the first IMF component often contains the highest frequency component of the original signal. The first three IMFs obtained from the original acceleration response time history at the first floor of the building under sinusoidal excitation and impulse excitation and their local zooms around the damage time instant are plotted in Fig. 4 and Fig. 5,

respectively. Similar observations can be made, that is, the local zoom of the first IMF is quite similar to the local portion of the corresponding acceleration response time history and the signal discontinuity is reserved in the first IMF only.

To extract inherent signal feature due to sudden damage from the signal discontinuity in either the original acceleration response time history or the first IMF of the original time history, the acceleration responses of the building under each type of excitation are computed for a sudden reduction of stiffness at the first story with different damage levels and damage time instants. Signal discontinuity patterns are then searched from extensive computed results, and all the possible patterns are plotted in Fig. 6. It can be seen from Fig. 6 that the signal discontinuity due to sudden stiffness change at the damage time instant t_i possesses two common distinct features: (1) the amplitude of acceleration signal \ddot{y} jumps up or down considerably from the damage time instant t_i to the time instant t_{i+1} ; and (2) the absolute values of signal slope at the time instant t_{i-1} and the time instant t_{i+1} are much smaller than that at the damage time instant t_i . These two features are the same as those observed from the SDOF system.

3.3 New damage index

In considering the aforementioned two signal discontinuity features and having an index more sensitive to sudden damage, a damage index, DI_i , is defined to reflect the signal discontinuity due to sudden damage at the time instant t_i

$$DI_i = |(K_i - K_{i-1}) + (K_i - K_{i+1})| = |2K_i - K_{i-1} - K_{i+1}| \quad (k = 2, 3, \dots, n-1) \quad (17)$$

This damage index is computed in the time domain and it is an instantaneous index suitable for online structural health monitoring application. Furthermore, the damage indices, DI_{i-1} and DI_{i+1} , at the time instants t_{i-1} and t_{i+1} can be calculated by

$$DI_{i-1} = |2K_{i-1} - K_{i-2} - K_i| \quad (18)$$

$$DI_{i+1} = |2K_{i+1} - K_i - K_{i+2}| \quad (19)$$

In consideration of Eq. (17), the summation of the damage indices, DI_{i-1} and DI_{i+1} , at the time instants t_{i-1} and t_{i+1} is approximately equal to the damage index DI_i at the damage time instant t_i , that is

$$DI_{i-1} + DI_{i+1} \approx DI_i \quad (20)$$

As a result, a common damage index pattern consists of one relatively large damage index DI_i at the damage time instant t_i and two relatively small indices DI_{i-1} and DI_{i+1} , satisfying Eq. (20), at the time instants t_{i-1} and t_{i+1} as shown in Fig. 7. The damage index at any other time instant without sudden stiffness reduction should be very small. This damage index pattern can help exclude some false damage indices. Furthermore, the linear relationship between the proposed damage index and the sudden stiffness reduction still remains.

$$DI_i = |2K_i - K_{i-1} - K_{i+2}| \approx |2K_i| \propto |K_i| \propto |\Delta k| \quad (21)$$

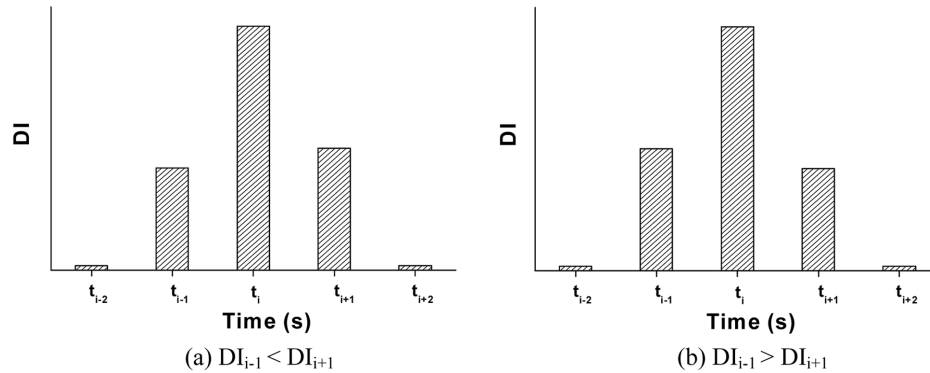


Fig. 7 Damage index patterns around damage time instant

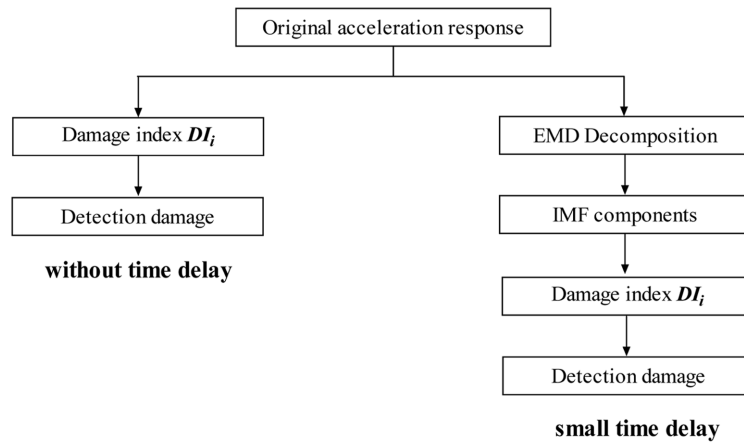


Fig. 8 Two detection approaches for sudden damage

3.4 Two damage detection approaches

Based on the above discussions, two damage detection approaches can be proposed to detect sudden damage of a structure in the time domain. One is to analyze the original acceleration response time history directly to obtain the variation of damage index with time, from which the damage event can be identified. The other is to use the EMD without intermittency check to decompose the original acceleration response time history to obtain its first IMF component. The variation of damage index with time is then computed basing on the first IMF to determine the damage event. The general steps involved in each damage detection approach are shown in Fig. 8. Clearly, the first approach can be implemented in an online health monitoring system without any time delay while the second approach needs a time history of certain length to execute the EMD and accordingly small time delay is unavoidable in terms of online damage detection. Nevertheless, the second approach gains an additional insight into the feature of sudden damage. Moreover, in conjunction with the Hilbert transform the second approach can provide other information on damage in the time-frequency domain as done by Yang *et al.* (2004).

4. Numerical example

4.1 Damage time instant and damage location

To examine the feasibility of the proposed damage index and damage detection approaches for identifying damage time instant and location, the acceleration responses of the aforementioned five-story shear building to the seismic excitation are computed. The building is subject to a 20% sudden stiffness reduction at time $t = 6.0$ second in the first story of the building only. The time step used in the computation is 0.002 second. The two approaches are then applied respectively to the acceleration response of each floor to calculate the damage index. Fig. 9(a) to Fig. 9(e) show variations of damage index with time for each floor of the building under the seismic excitation, obtained by the first approach without using EMD. Fig. 9(f) to Fig. 9(j) display the same quantities but they are obtained by the second approach using the first IMF. It can be seen that no matter which approach is used, the damage index of the first floor is very large only at time $t = 6.0$ second, which is exactly the moment when the stiffness of the first story is suddenly reduced by 20%. The damage indices of the first floor at all other time instants (except for time $t = 5.998$ second, 6.0

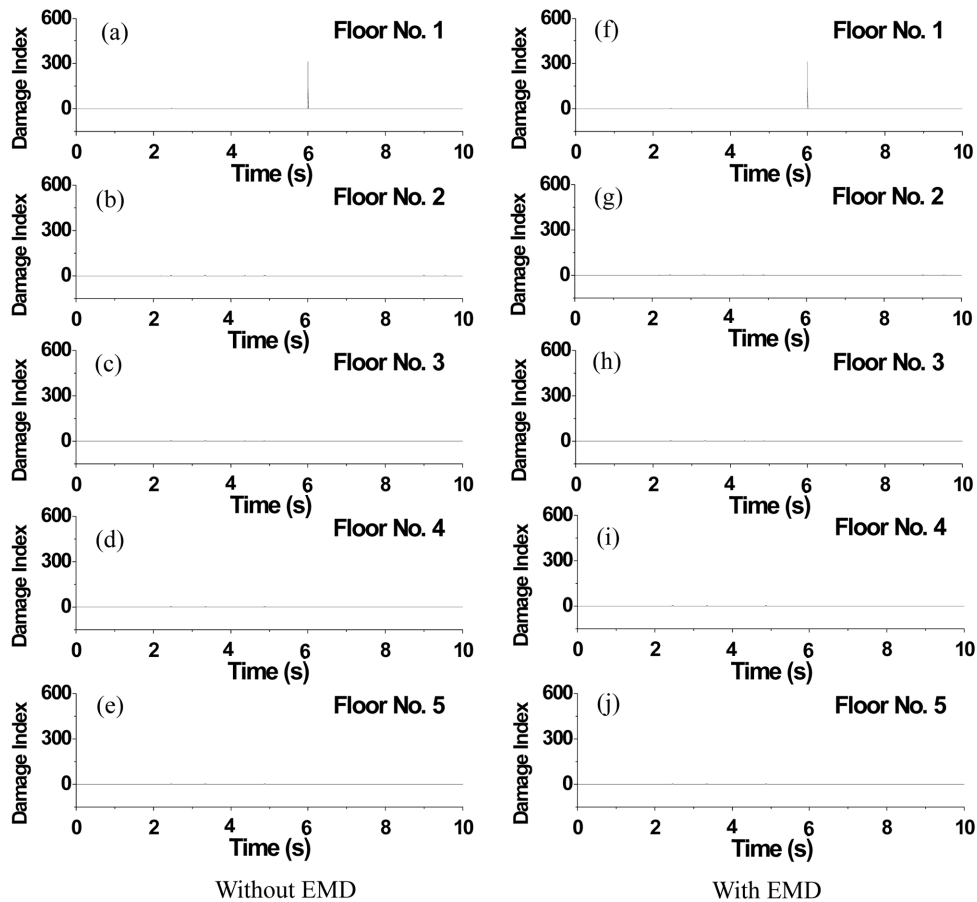


Fig. 9 Variations of damage index with time (seismic excitation)

second, and 6.002 second) are very small so that the damage index at time $t = 6.0$ second looks like a spike. Therefore, the damage time instant can be easily identified by the occurrence time of the sharp damage index. Let us now compare the variation of damage index of the first floor (Fig. 9(a)) with those of the second, third, fourth, and fifth floors of the building (Fig. 9(b) to Fig. 9(e)). The sharp damage index appears clearly only in the first floor, and no sharp damage index emerges in other floors. Therefore, by analyzing the distribution of sharp damage index along the height of the building, the damage location can be easily identified at the first story of the building. The same conclusion with respect to the damage location can be reached using the second approach with the first IMF as shown in Fig. 9(f) to Fig. 9(j).

The variations of damage index with time for each floor of the building are shown in Fig. 10 for sinusoidal excitation and in Fig. 11 for impulse excitation using the two approaches. The building is subject to the same damage severity at the first story only but it occurs at time $t = 6.0$ second for sinusoidal excitation and at time $t = 0.2$ second for impulse excitation. Again, the sharp damage index appears only at the moment of sudden stiffness reduction at the first floor. Thus, the damage time instant and location can be easily captured from the observed occurrence time of the sharp damage index and its distribution along the height of the building. As expected, for the building under a given excitation the magnitude of the sharp damage index obtained by the first approach is

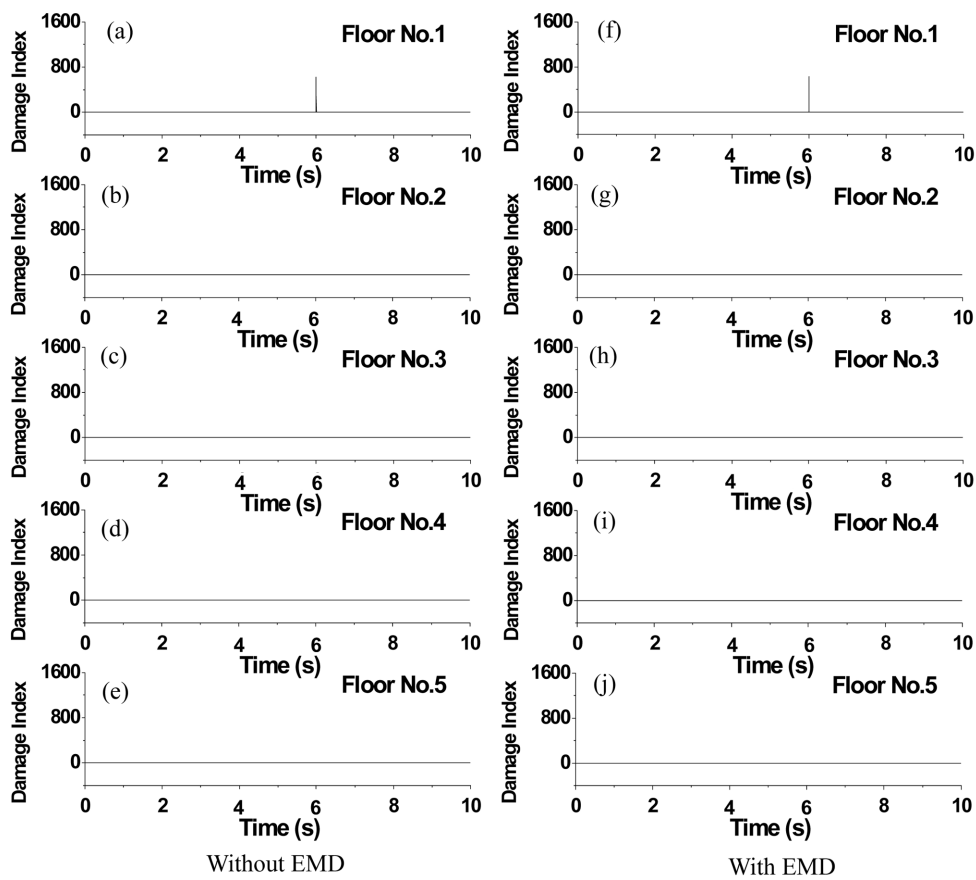


Fig. 10 Variations of damage index with time (sinusoidal excitation)

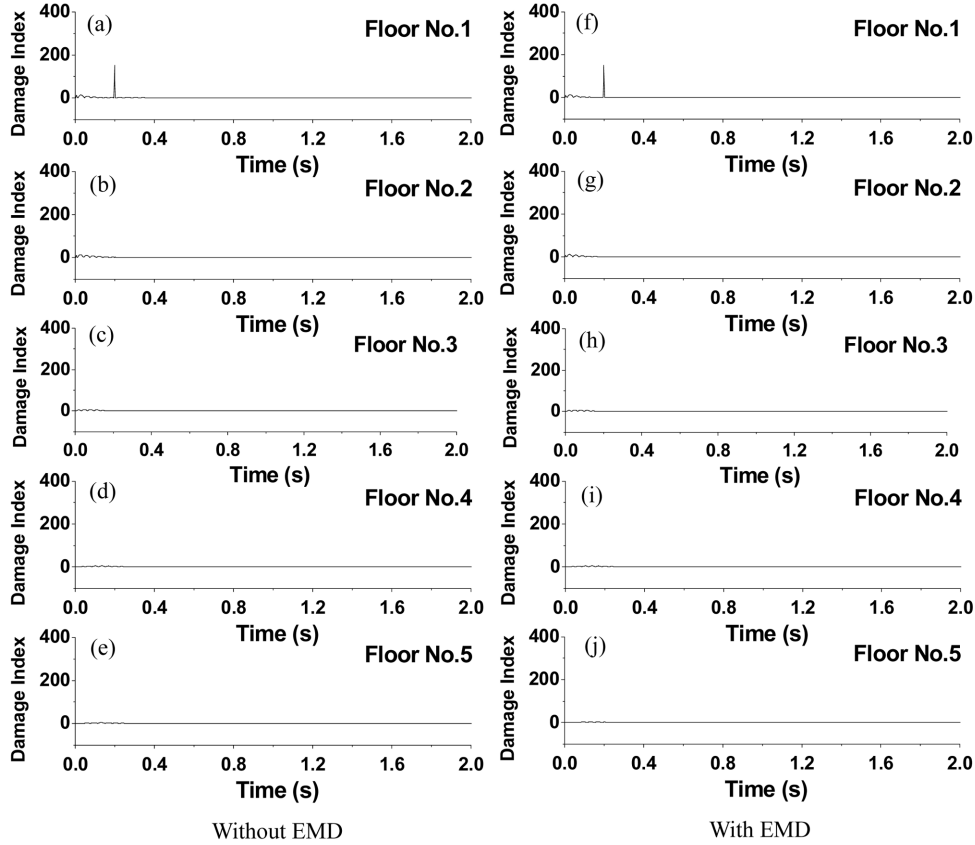


Fig. 11 Variations of damage index with time (impulse excitation)

Table 2 Damage indices around damage time instant

Frequency (Hz)	DI_{i-2}	DI_{i-1}	DI_i	DI_{i+1}	DI_{i+2}	ΔDI_i
El Centro earthquake	1.083	160.44	313.97	152.53	0.191	0.32%
Sinusoidal excitation	0.011	291.58	625.27	329.14	1.223	0.73%
Impulse excitation	0.690	70.42	152.07	80.78	0.319	0.57%

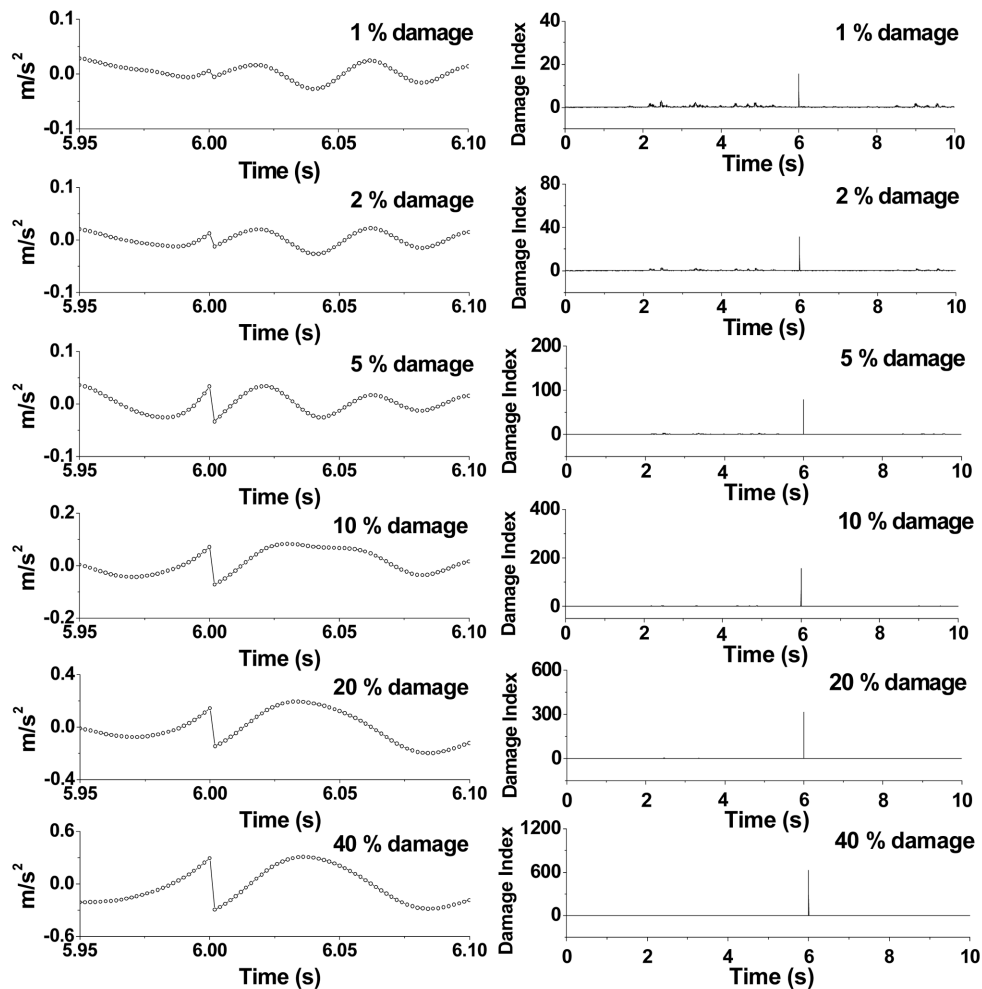
almost the same as that obtained by the second approach. To check the relationship expressed by Eq. (20), the damage indices computed around the damage time instant for each type of excitation are listed in Table 2. In Table 2, the item ΔDI_k is defined as follows

$$\Delta DI_k = \frac{|DI_{k-1} + DI_{k+1} - DI_k|}{|DI_k|} \cdot 100\% \tag{22}$$

Clearly, Eq. (22) exists for the three excitation cases studied here and the damage index patterns are consistent with those presented in Fig. 7. However, it can be observed that the magnitude of sharp damage index is different for the same building under different types of excitation. The magnitude of sharp damage index depends on many factors such as type of excitation, damage time instant and damage severity, which will be discussed subsequently.

4.2 Sensitivity of damage index to damage severity

To further examine the feasibility of the proposed damage index and damage detection approaches, parameter studies are executed in this section to find the sensitivity of damage index to damage severity. The first floor of the five-story building is supposed to suffer different levels of sudden stiffness reduction but the sudden reduction occurs at the same time. Listed in Table 1 are the damage severities and the corresponding five natural frequencies of the building before and after the sudden damage. The results presented in Table 1 indicate that the stiffness reduction in the first story of the building affects mainly on lower natural frequencies. It is noted that if the stiffness reduction in the first floor is less than 20%, the maximum frequency change is no more than 5%. Since the proposed two approaches give almost the same results, only the results from the second approach using the first IMF are presented and discussed in the following.



(a) Signal discontinuity of the first IMF (b) Damage index of the first floor

Fig. 12 Sensitivity of damage index to damage severity (seismic excitation)

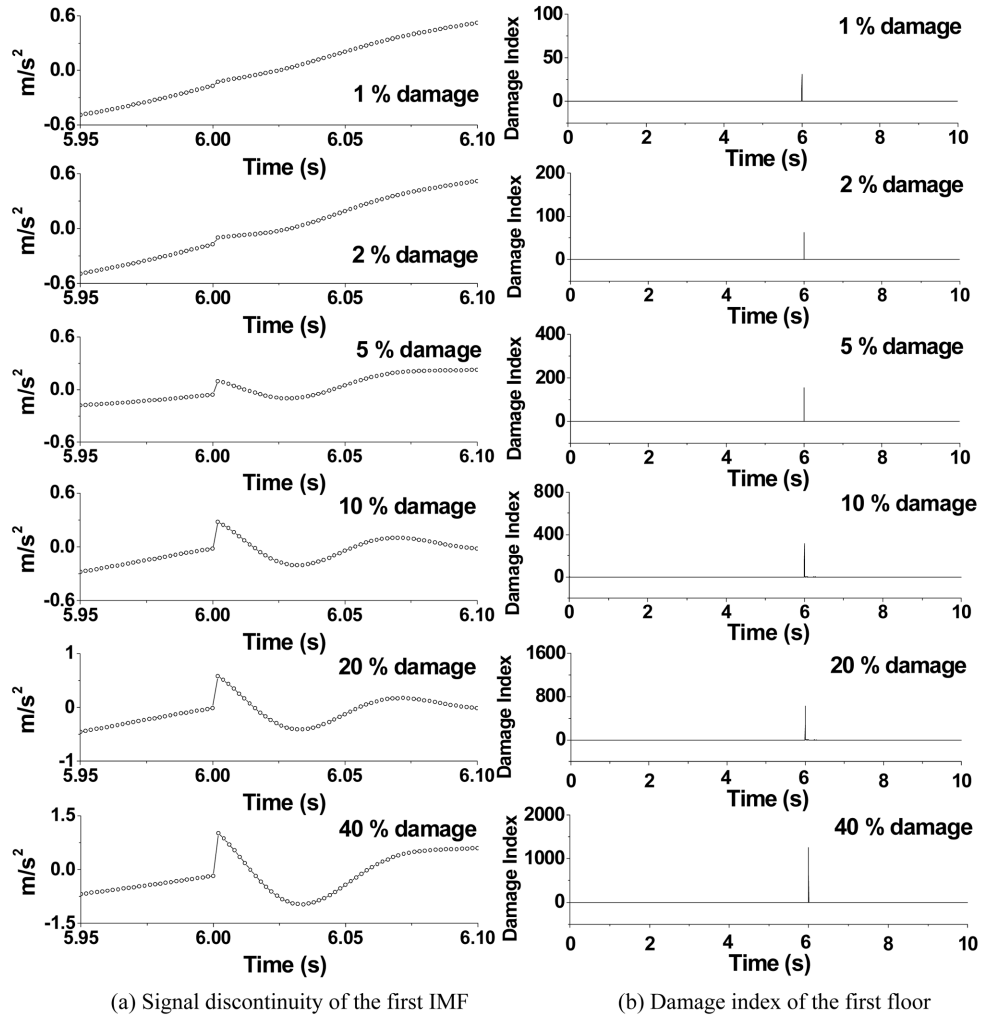


Fig. 13 Sensitivity of damage index to damage severity (sinusoidal excitation)

The 0.15 second portion of the first IMF of the acceleration response at the first floor of the building to the seismic excitation is plotted in Fig. 12 for the sudden stiffness reduction from 1% to 40%. The variations of damage index with time obtained from the first IMF are also depicted in the same figure. It can be seen that even for small damage event such as 1% to 5% sudden stiffness reduction, the proposed approach can easily capture the damage features for noise free situation. The magnitude of sharp damage index also increases with increasing damage severity. Similar results are also obtained for the building subject to sinusoidal excitation as shown in Fig. 13. For the building under impulse excitation, however, the proposed approaches may not give satisfactory results for the building with small damage event (1% to 2% sudden stiffness reduction) as shown in Fig. 14. This is because the signal fluctuates significantly immediately after the initial velocity. Nevertheless, if the damage index pattern shown in Fig. 7 and expressed by Eq. (20) is utilized with the following criterion

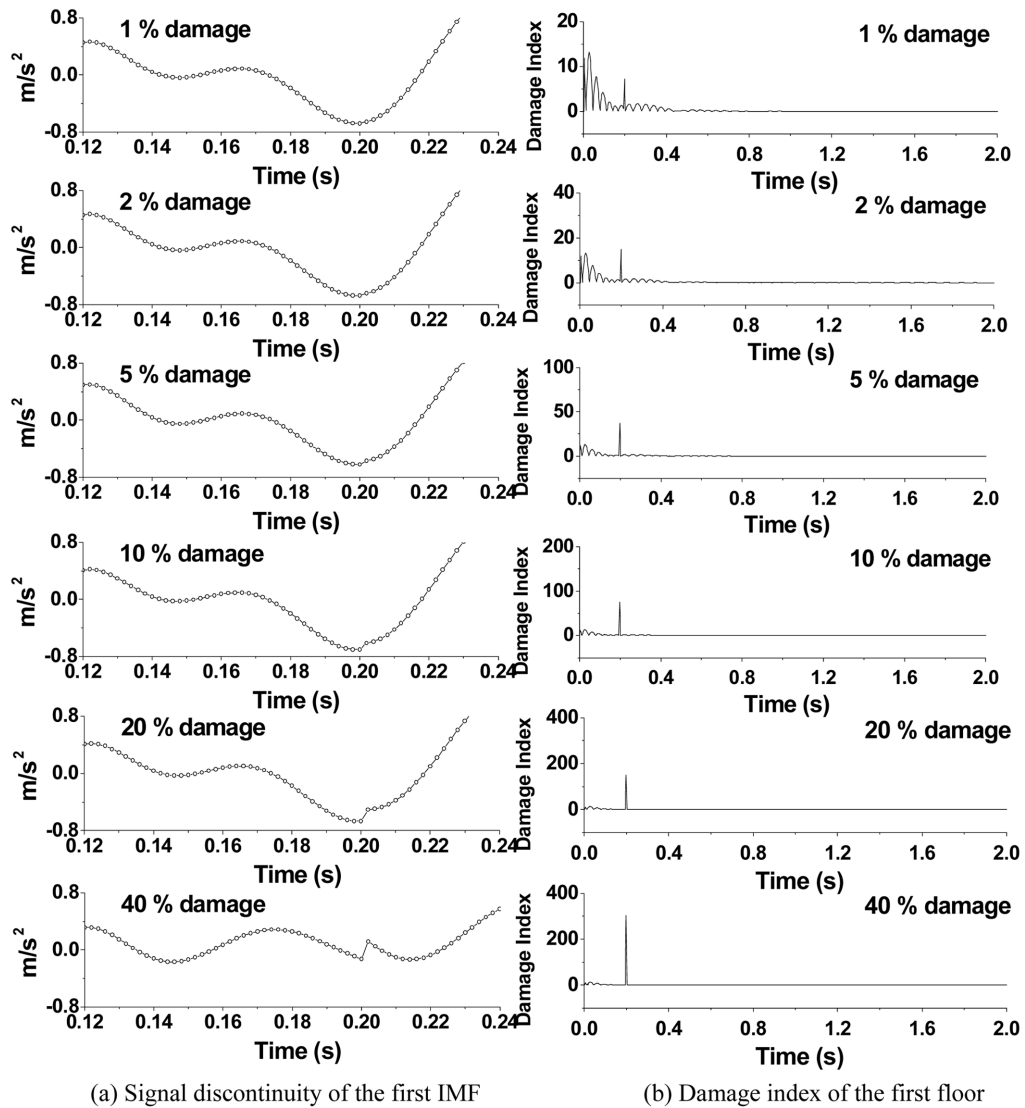


Fig. 14 Sensitivity of damage index to damage severity (impulse excitation)

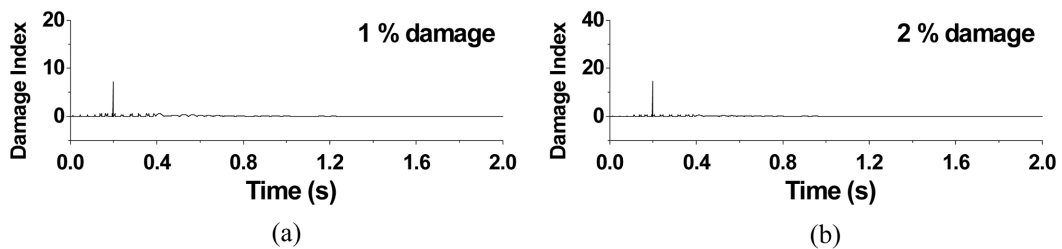


Fig. 15 Improved minor damage detection (impulse excitation)

$$DI_i = \begin{cases} 0 & (\Delta DI_i > T) \\ DI_i & (\Delta DI_i \leq T) \end{cases} \quad (23)$$

the damage detection results will be improved for the small damage events as shown in Fig. 15. In Eq. (23), T is the threshold value and it is 0.2 used to obtain the results in Fig. 15.

4.3 Relationship between damage index and damage severity

The magnitudes of sharp damage index corresponding to different damage severities in the first story of the building subject to seismic, sinusoidal and impulse excitations are computed and listed in Table 3 for the first approach without using EMD and in Table 4 for the second approach basing on the first IMF. They are also plotted in Fig. 16 together with a linear fit in which x represents damage severity (stiffness reduction) and y represents damage index. It can be seen that the relationship between damage index and damage severity is quite linear for the building under either seismic or sinusoidal or impulse excitation. For a given external excitation, the larger the stiffness reduction, the larger is the damage index. Also for a given external excitation, the linear relationship obtained by the first approach without using EMD is very close to that obtained by the second

Table 3 Relationship between damage index and damage severity (without EMD)

Damage severity	0%	1%	2%	5%	10%	20%	40%
DI (seismic excitation)	0.001	15.839	31.597	78.868	157.63	315.09	629.72
DI (sinusoidal excitation)	0.004	31.283	62.560	156.38	312.72	625.27	1249.9
DI (impulse excitation)	0.002	7.384	15.011	37.890	76.015	152.24	304.57

Table 4 Relationship between damage index and damage severity (with EMD)

Damage severity	0%	1%	2%	5%	10%	20%	40%
DI (seismic excitation)	0.002	15.592	31.323	78.270	157.03	313.97	628.23
DI (sinusoidal excitation)	0.005	31.284	62.559	156.37	312.71	625.27	1249.8
DI (impulse excitation)	0.001	7.211	14.852	37.714	75.860	152.07	302.42

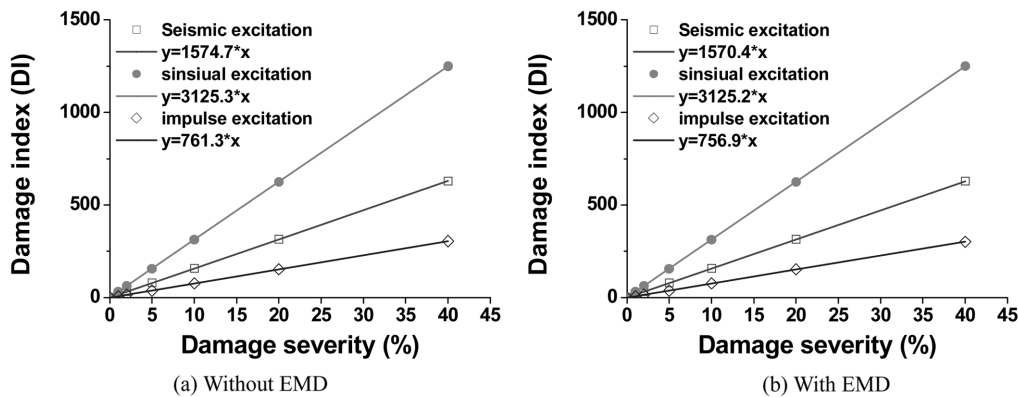


Fig. 16 Relationship between damage index and damage severity

approach basing on the first IMF. However, the slope of the linear fit is different for the building under different excitations. This creates a problem for the sole determination of damage severity. One possible way of solving this problem is to measure external excitation in addition to structural responses. The proposed approach is then used to find the damage time instant and damage location from the measured structural responses. Afterwards, the measured external excitation is input to the structural model with a sudden stiffness reduction at the identified damage location and at the identified damage time instant to determine the slope of the linear relationship between the damage severity and damage index. The linear relationship can finally used to determine the damage severity in the actual structure in terms of the damage index identified from the actual structure.

4.4 Effects of noise intensity and frequency range

To apply the proposed approaches to health monitoring and damage detection of real structures, many practical issues need to be addressed. The effect of measurement noise, which contaminates structural responses, on the detection of real structural damage is a key issue. Yang *et al.* (2004) reported that the damage spike identified from the first IMF component using the intermittency check could be weakened by measurement noise, and strong measurement noise could lead to the failure of damage detection. In consideration that the sudden damage event introduces a high frequency component to acceleration responses of a structure, the effects of both measurement noise intensity and frequency range on the damage detection using the proposed approaches are investigated in this study. The measurement noise in structural response is assumed to be a random white noise. Three frequency ranges are considered: (1) white noise with frequency range from 0 to 50 Hz; (2) white noise with frequency range from 0 to 100 Hz; and (3) white noise with frequency range from 0 to 250 Hz. The measurement noise intensity is defined as

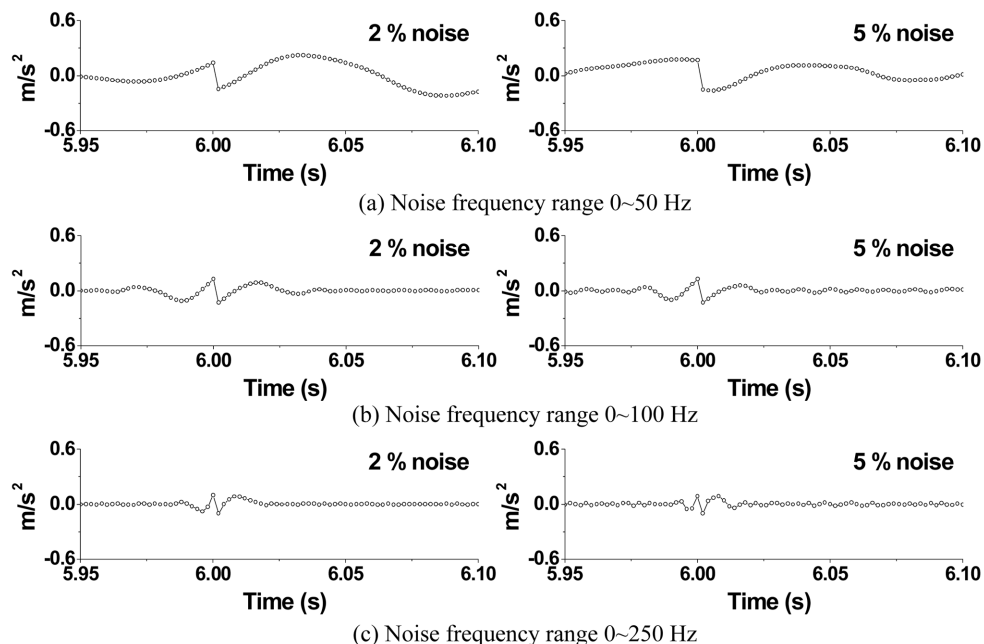


Fig. 17 First IMF components of contaminated acceleration responses with sudden damage (seismic excitation)

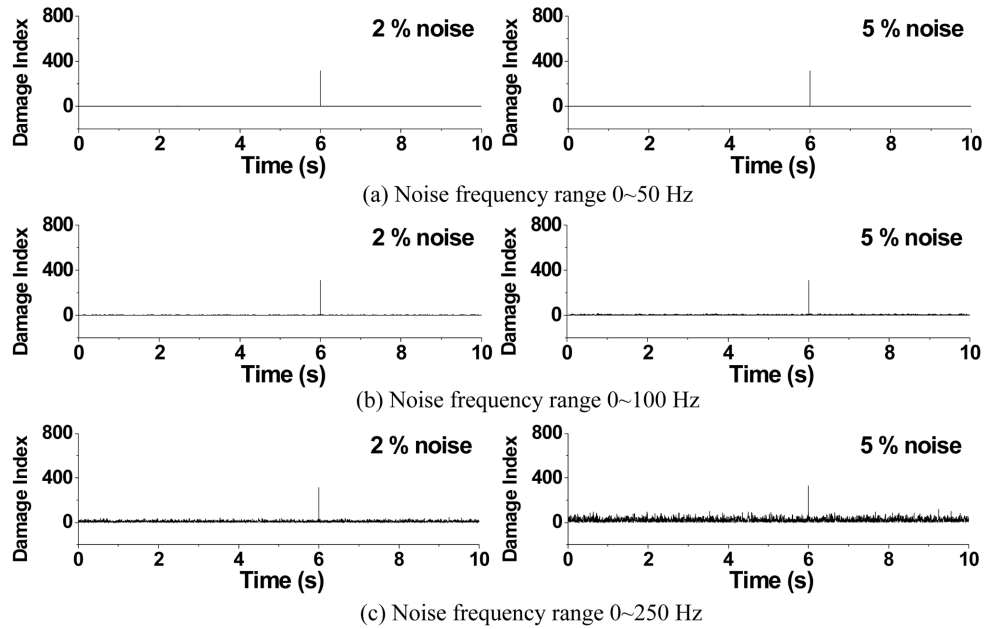


Fig. 18 Damage index from contaminated acceleration responses with sudden damage (seismic excitation)

$$\text{Noise intensity} = \frac{\text{RMS}(\text{noise})}{\text{RMS}(\text{signal})} \times 100\% \quad (24)$$

Displayed in Fig. 17 are the 0.15 second zooms of the first IMFs of the contaminated acceleration responses of the five story building at the first floor under the seismic excitation for two noise intensities and three noise frequency ranges. The sudden stiffness reduction in the first story of the building is 20%. It can be seen that with increasing noise frequency range, the acceleration response of the first floor becomes more fluctuating and the signal discontinuity at the damage time instant gets weak. The variations of the corresponding damage index obtained by using the second approach with the first IMF are provided in Fig. 18 for the seismic excitation case. Clearly, the proposed approach can still identify the damage time instant from the contaminated acceleration response of the building at the first floor for the designated two noise intensities and three noise frequency ranges. Furthermore, by checking the spatial distribution of sharp damage index along the height of the building, the proposed approach can also identify the damage location from the contaminated acceleration response for the designated two noise intensities and three noise frequency ranges. The same results are obtained for the sinusoidal excitation case, as shown in Fig. 19. However, for the impulse excitation case, the proposed approach fails to identify the damage time instant and damage location when the noise frequency range is from 0 to 250 Hz and the noise intensity is 5%, as shown in Fig. 20.

The effects of measurement noise on the magnitude of damage index are assessed and the results are listed in Table 5 for seismic excitation, in Table 6 for sinusoidal excitation, and in Table 7 for impulse excitation. It can be seen that as long as the damage event can be identified, the magnitude of damage index remains almost the same for the designated two noise levels and three noise frequency ranges no matter which approach is used. This indicates that the effect of measurement noise on the magnitude of damage index is small. This is probably because the damage index

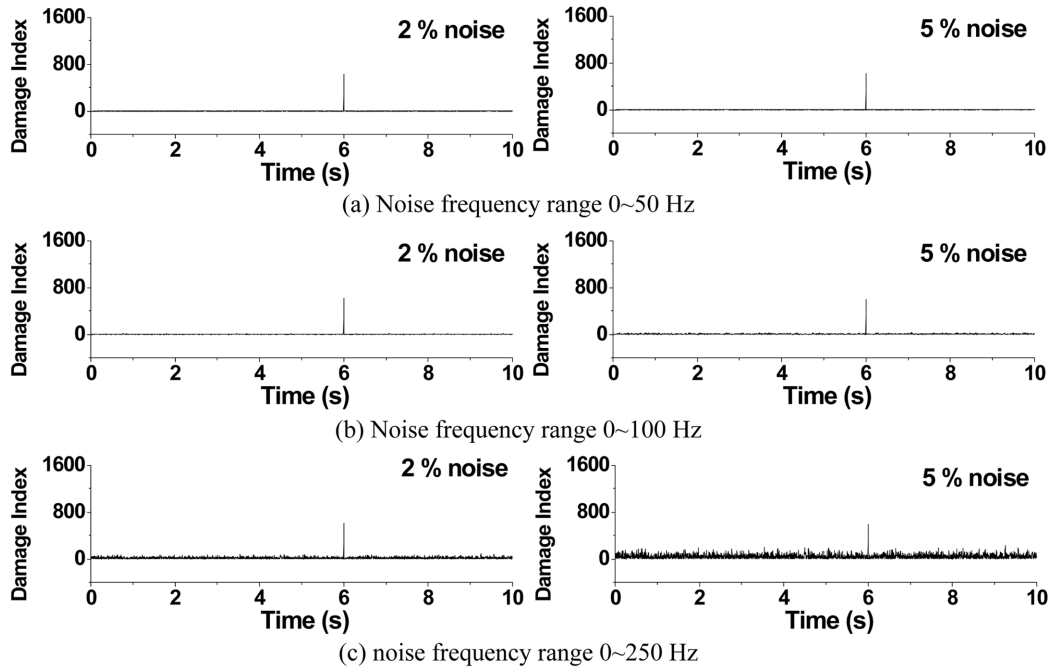


Fig. 19 Damage index from contaminated acceleration responses with sudden damage (sinusoidal excitation)

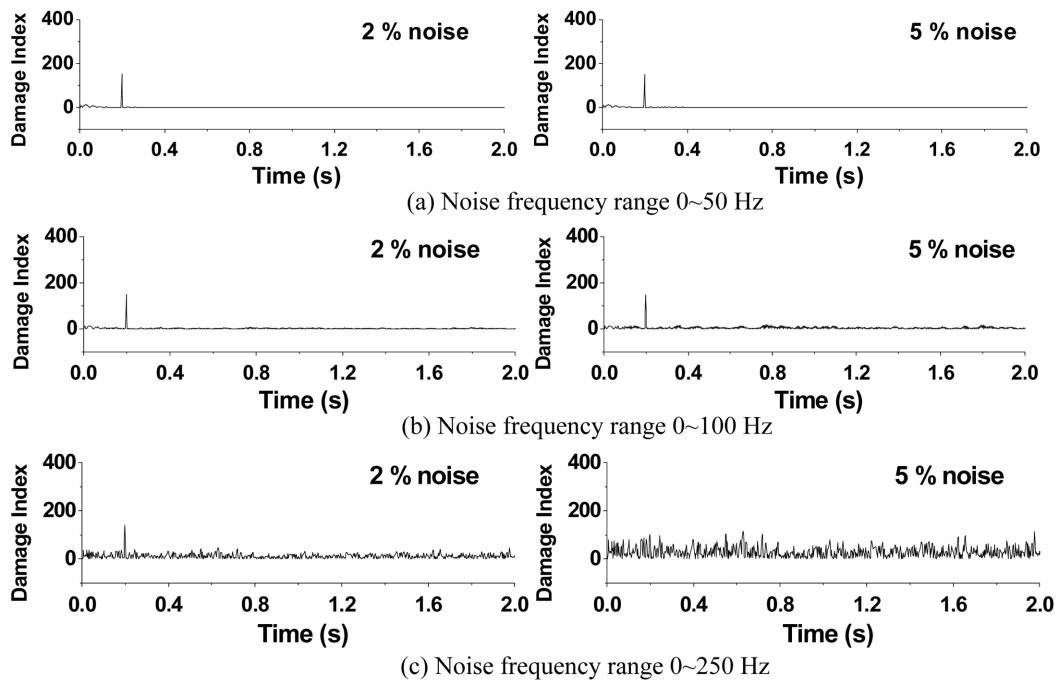


Fig. 20 Damage index from contaminated acceleration responses with sudden damage (impulse excitation)

Table 5 Noise effects on damage index magnitude (seismic excitation)

Noise level	Noise frequency range		
	0~50 Hz	0~100 Hz	0~250 Hz
without EMD			
No noise	315.09	315.09	315.09
2% noise	315.22 (-0.04%)	317.14 (-0.65%)	322.26 (2.28%)
5% noise	315.41 (0.10%)	320.22 (1.63%)	333.01 (5.69%)
with EMD			
No noise	313.98	313.98	313.98
2% noise	313.90 (-0.03%)	312.31 (-0.53%)	313.04 (-0.30%)
5% noise	315.34 (0.43%)	311.21 (-0.88%)	301.55 (-3.95%)

Table 6 Noise effects on damage index magnitude (sinusoidal excitation)

Noise level	Noise frequency range		
	0~50 Hz	0~100 Hz	0~250 Hz
without EMD			
No noise	625.26	625.26	625.26
2% noise	625.00 (-0.04%)	614.57 (-1.71%)	610.84 (-2.31%)
5% noise	624.02 (-0.20%)	598.55 (-4.27%)	589.21 (-5.76%)
with EMD			
No noise	625.27	625.27	625.27
2% noise	625.04 (-0.04%)	618.85 (-1.03%)	612.11 (-2.11%)
5% noise	621.48 (-0.61%)	602.28 (-3.68%)	593.08 (-5.15%)

Table 7 Noise effects on damage index magnitude (impulse excitation)

Noise level	Noise frequency range		
	0~50 Hz	0~100 Hz	0~250 Hz
without EMD			
No noise	152.23	152.23	152.23
2% noise	152.00 (-0.15%)	150.59 (-1.08%)	143.81 (-5.54%)
5% noise	151.65 (-0.79%)	148.13 (-2.70%)	-
with EMD			
No noise	152.073	152.073	152.073
2% noise	151.83 (-0.15%)	150.37 (-1.10%)	143.70 (-5.51%)
5% noise	150.87 (-0.79%)	147.94 (-2.70%)	-

defined here is an instantaneous damage index. The further numerical simulation indicates that the damage can be effectively identified for 20% sudden stiffness reduction even with 80% noise intensity as long as the noise frequency range is not higher than 50 Hz. However, if the noise frequency range is from 0 to 250 Hz, the reliability of damage detection using the proposed approaches remarkably deteriorates with the increase of noise intensity.

5. Comparison with WT and EMD based approaches

To further assess the performance of proposed detection approaches, the wavelet-transform (WT) and the empirical mode decomposition (EMD) with intermittency check are applied to the same problem without and with noise contamination. All the damage cases remain the same as those investigated by the proposed approach. Three noise frequency ranges and two noise intensities, which are the same as those used for assessing the proposed approach, are repeated. Since the damage detection efficiency of wavelet based approach depends on the properties of mother wavelet used, such as, wavelet vanishing moments and support length, three different Daubechies wavelets db1, db2 and db4 are utilized to detect the structural sudden damage of the building subject to sinusoidal, seismic and impulse excitation, respectively (Hera and Hou 2004). The selected db1, db2 and db4 wavelets have the vanishing moments 1, 2 and 4, respectively, and the corresponding support lengths are 1, 3 and 7, respectively.

The proposed approach, the WT and the EMD with intermittency check all could deal with the concerned damage detection problem but from different viewpoints. The WT and EMD based approaches decompose the original signal into several components and detect damage event from the component with the highest frequency. As a result, these approaches may encounter some difficulties if the frequency components of an original signal are wide enough to overlap the high frequency damage signal or the energy of damage is too small to be extracted from the original signal. Furthermore, the selection of intermittency check frequency used with EMD is arbitrary, which may cause some inconvenience and inaccuracy in detection. The proposed approach, on the other hand, detects signal discontinuity at the damage instant directly and it does not need to decompose the signal. Therefore, its detection efficiency is not remarkably affected by the high frequency components of the original signal compared with the WT and EMD based approaches.

The numerical results demonstrate that the WT based approach using all the three Daubechies wavelets can accurately detect the damage instant of the building subject to sinusoidal excitation. For the seismic excitation case, the WT using db1 wavelet fails to detect damage instant while the

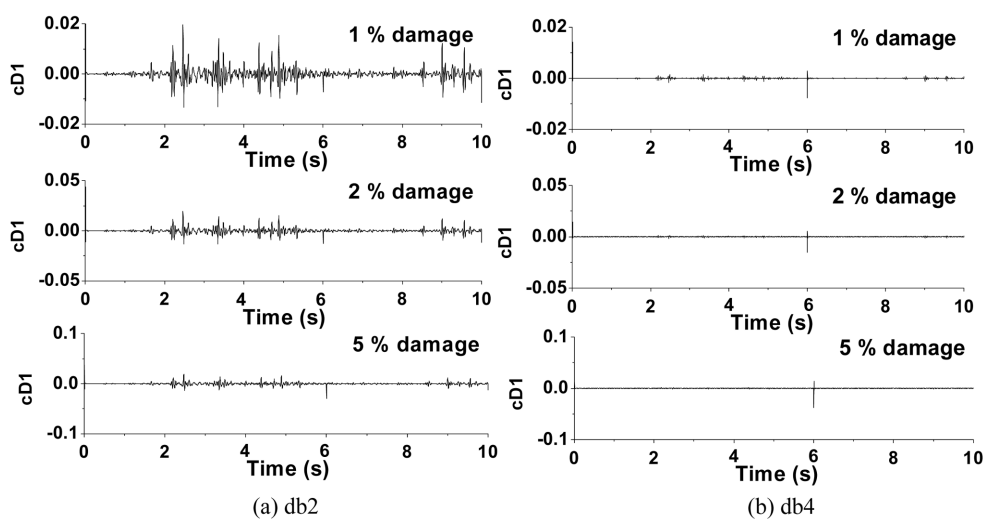


Fig. 21 Damage detection using different db wavelets under seismic excitation

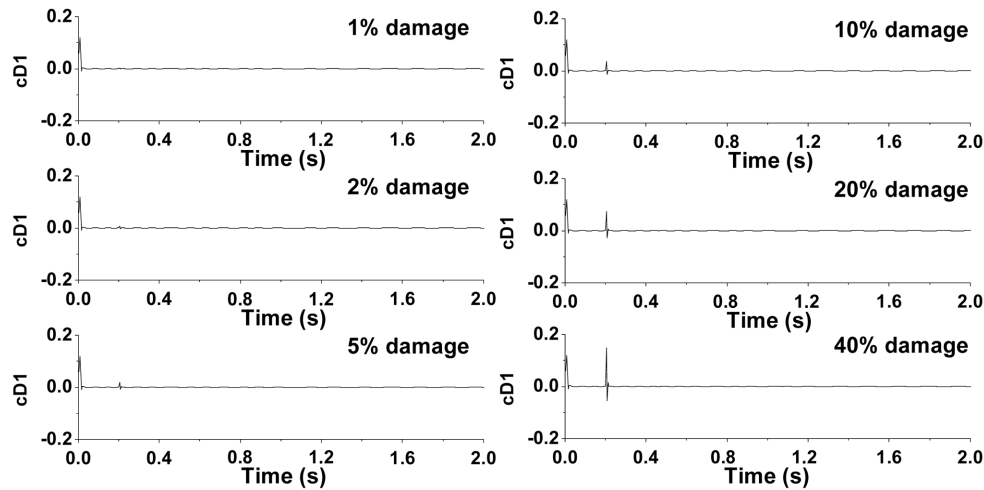


Fig. 22 Damage detection using db4 wavelet under impulse excitation

WT using db2 can detect damage only when the damage extent is large enough. The wavelet coefficient details in level 1 ($cD1$) obtained by applying the WT with db2 and db4 to the acceleration response time histories at the first floor of the building under seismic excitation are depicted in Fig. 21 for small damage extent. It can be seen that when the damage extent is small, the db2 wavelet fails to work while the db4 wavelet with longer support length can effectively detect damage. As for the impulse excitation case, the numerical results show that only the WT using db4 wavelet can detect the damage instant. This is because the longer the wavelet support length, the finer is the frequency components which is especially useful in detecting high frequency damage signal. Furthermore, the numerical results show that the WT using db4 can detect various damage extents of the building under sinusoidal and seismic excitation. However, the satisfactory detection can not be obtained for impulse excitation case with minor damage extents as shown in Fig. 22. Actually, for the building subject to sinusoidal and seismic excitations, the acceleration response spectra have relatively low frequency components but the impulse excitation caused acceleration response spectrum has much wider frequency range which may overlap high frequency damage signal leading to detection fail. Furthermore, the minor damage event may cause small signal energy and conveys minor damage information. This makes the wavelet coefficients from the original signal to the selected mother wavelet be too small to form obvious peaks and reflect damage event. Because of this, the mother wavelets with higher vanishing moments and longer support length (such as db8 or db10) also cannot improve the damage detection efficiency.

The acceleration responses of the building with 20% damage at its first floor under the sinusoidal, seismic and impulse excitation are analyzed, respectively, with measurement noise included. The noises are introduced with two noise intensities and three noise frequency ranges as used before. The results reveal that the WT based approach can identify the damage time instant and location from the contaminated acceleration responses for sinusoidal and seismic excitation cases. For impulse excitation case, however, the WT fails to identify the damage time instant and damage location when the noise frequency range is from 0 to 250 Hz and the noise intensity is 5%, as shown in Fig. 23. Obviously, the detection accuracy will decrease with the increase of noise intensity, which is the same as observed when using the proposed approach.

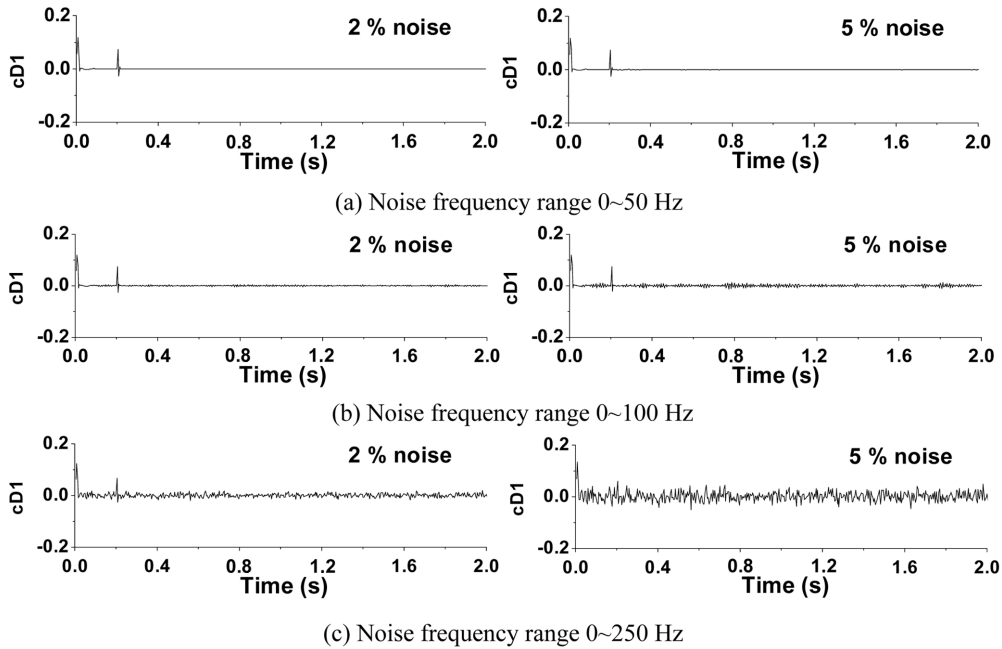


Fig. 23 Detection results from contaminated acceleration responses using db4 wavelet (impulse excitation)

The EMD with intermittency check is also applied to the same building with different damage severities and noise cases subject to three excitations. Only a summary of the results is given here because of limitation of space. The numerical results demonstrate that the efficiency of EMD with intermittency check is quite similar to the WT in sinusoidal and seismic excitation cases. The detection efficiency in impulse excitation case is worse than that identified by the WT based approach for minor damage event. The selection of intermittency check frequency will affect the spike amplitude, and as a result there is no a quantitative relationship between spike amplitude and damage extent (sudden stiffness reduction).

In summary, the proposed approach, the WT and the EMD with intermittency check all could deal with the concerned damage detection problem but the proposed approach can provide more accurate results than other two approaches in impulse excitation case with measurement noise for small damage events. Furthermore, both the numerical study and the experimental investigation demonstrate that the relationship between damage spike amplitude and damage severity could not be given by either the WT or the EMD with intermittency check. The proposed approach, however, could provide a linear relationship between damage index and damage severity. This has been theoretically proved using a SDOF system under impulse excitation. The numerical simulation results from MDOF systems under sinusoidal, seismic and impulse excitations also demonstrate the linear relationship between the damage index and damage severity. However, if the noise frequency range is further widened, the detection accuracy using either the proposed approach, or the WT or the EMD remarkably deteriorates with the increase of noise intensity. Thus, the effective noise eliminating techniques for detecting sudden stiffness change need further investigation.

6. Conclusions

The features of signal discontinuity in acceleration response time histories of a structure due to sudden stiffness reduction have been examined and a new damage index has been proposed. Two damage detection approaches in terms of the proposed damage index have been put forward for the online and offline detection, respectively, of damage time instant, damage location, and damage severity. Extensive numerical simulations have been executed on a five-story shear building to evaluate the performance of proposed damage detection approaches. Major observations from this study are summarized as follows:

- (1) The proposed two detection approaches can accurately identify the damage time instant and damage location due to a sudden stiffness reduction of the building in terms of the occurrence time and spatial distribution of sharp damage indices along the height of the building.
- (2) The proposed damage index is linearly proportional to damage severity but the slope of linear function depends on external excitation and damage time instant. A possible way of determining damage severity has been suggested using the calibrated structural model and the measured excitation.
- (3) The proposed two detection approaches both are applicable to the building under either seismic excitation or sinusoidal excitation or impulse excitation. The approach without using empirical mode decomposition (EMD) is suitable for online health monitoring and damage detection systems while the approach basing on the EMD can provide additional sights on structural damage features in the time-frequency domain in terms of Hilbert transform. The online damage detection defined here means that damage event can be detected without any time delay. The WT and the EMD should apply to a time history of certain length and then decomposed it into several components and detect damage event from the component with highest frequency. Therefore, the WT and the EMD detect damage event with certain time delay. Only when this time delay is small, one may also call the WT and the EMD online monitoring approaches.
- (4) The proposed two approaches can identify the damage time instant and damage location from the contaminated acceleration responses of the building if the upper bound of noise frequency range is less than 100 Hz. If the noise frequency range is from 0 to 250 Hz, the reliability of damage detection using the proposed approaches remarkably deteriorates with the increase of noise intensity. As long as the damage event can be identified, the magnitude of damage index remains almost the same for different noise intensities and frequency ranges no matter which approach is used.
- (5) The extensive comparison of the proposed approaches with the wavelet transform (WT) and the empirical model decomposition (EMD) with intermittency check demonstrates that all three approaches could extract the damage information from the original signal. However, the proposed approach could detect minor damage event with measurement noise caused by impulse excitation. The proposed approach could also provide a linear relationship between damage index and damage severity.

It should be pointed out that some structures may experience a transient high frequency acceleration response due to other reasons than sudden structural damage. In such a case, a full understanding of the actual reasons and the feature of the associated signals is necessary before applying the proposed approaches.

Acknowledgements

The writers are grateful for the financial support from The Hong Kong Polytechnic University through a PhD studentship to the first writer and through its Area of Strategic Development Programme in Structural Health Monitoring and Damage Detection to the second writer. Sincere thanks should go to Dr J. Chen from Tongji University, China, for his beneficial discussions with the writers.

References

- Hera, A. and Hou, Z. (2004), "Application of wavelet approach for ASCE structural health monitoring benchmark studies", *J. Eng. Mech.*, ASCE, **130**(1), 96-104.
- Hou, Z. and Noori, M. (1999), "Application of wavelet analysis for structural health monitoring", *Proc. of 2nd Int. Workshop on Structural Health Monitoring*, Stanford Univ., Stanford, CA, 946-955.
- Hou, Z., Noori, M. and Amand, R.S. (2000), "Wavelet-based approach for structural damage detection", *J. Eng. Mech.*, ASCE, **126**(7), 677-683.
- Huang, N.E., Shen, Z. and Long, S.R. (1999), "A new view of nonlinear water wave: the Hilbert spectrum", *Annual Review Fluid Mech.*, **31**, 417-457.
- Huang, N.E., Shen, Z., Long, S.R., Wu, M.C. and Shih, H.H. (1998), "The empirical mode decomposition and Hilbert spectrum for nonlinear and nonstationary time series analysis", *Proc. of the Royal Society of London – Series A*, **454**, 903-995.
- Johnson, E.A., Lam, H.F., Katafygiotis, L.S. and Beck, J.L. (2000), "A benchmark problem for structural health monitoring and damage detection", *Proc. of 14th Engineering Mechanics Conf.* (CD Rom), ASCE, Reston, Va.
- Maity, D. and Tripathy, R.R. (2005), "Damage assessment of structures from changes in natural frequencies using genetic algorithm", *Struct. Eng. Mech.*, **19**(1), 21-42.
- Sohn, H., Farrar, C.R., Hemez, F.M., Shunk, D.D., Stinemates, D.W. and Nadler, B.R. (2003), "A review of structural health monitoring literature: 1996-2001", *Los Alamos National Laboratory Report*, LA-13976-MS.
- Sohn, H., Robertson, A.N. and Farrar, C.R. (2004), "Holder exponent analysis for discontinuity detection", *Struct. Eng. Mech.*, **17**(3-4), 409-428.
- Vincent, B., Hu, J. and Hou, Z. (1999), "Damage detection using empirical mode decomposition and a comparison with wavelet analysis", *Proc. of 2nd Int. Workshop on Structural Health Monitoring*, Stanford Univ., Stanford, CA, 891-900.
- Xu, Y.L. and Chen, J. (2004), "Structural damage detection using empirical mode decomposition: Experimental investigation", *J. Struct. Eng.*, ASCE, **130**(11), 1279-1288.
- Yang, J.N., Lei, Y. and Huang, N.E. (2001), "Damage identification of civil engineering structures using Hilbert-Huang transform", *Proc. of 3rd Int. Workshop on Structural Health Monitoring*, Stanford, CA, 544-553.
- Yang, J.N., Lei, Y., Lin, S. and Huang, N. (2004), "Hilbert-Huang based approach for structural damage detection", *J. Eng. Mech.*, ASCE, **130**(1), 85-95.